ACS OMEGA

Open Access

http://pubs.acs.org/journal/acsodf

Article

A Novel Role for Protein Tyrosine Phosphatase 1B in Alleviating Chondrocyte Senescence

Hui-Min Li,[#] Xianda Che,[#] Zhicheng Tong, Wei Wei,[*] and Chong Teng[*]

Cite This: *ACS Omega* 2024, 9, 27017−27029

Read Online

ACCESS | Metrics & More | Article Recommendations | Supporting Information

ABSTRACT: Osteoarthritis (OA) is a kind of arthritis that impairs movement and causes joint discomfort. Recent research has demonstrated a connection between cellular senescence and the degenerative processes of OA chondrocytes. In yeast and human cells, protein tyrosine phosphatase 1B (PTP1B) knockdown prolongs longevity; however, the function of PTP1B in chondrocyte senescence has not been investigated. The goal of the current investigation was to evaluate PTP1B's contribution to human OA chondrocyte senescence. The function of PTP1B and cellular senescence in the onset of OA was investigated and confirmed by using a combination of bioinformatics techniques, clinical samples, and *in vitro* experimental procedures. The RNA sequencing data pertinent to the OA were obtained using the Gene Expression Omnibus database. Function enrichment analysis, protein−protein correlation analysis, the construction of the correlation regulatory network, and an investigation into possible connections between PTP1B and cellular senescence in OA were all carried out using various bioinformatic techniques. Compared with healthy cartilage, PTP1B expression was increased in OA cartilage. According to a Pearson correlation study, cellular senescence-related genes, including MAP2K1 and ABL1, were highly correlated with PTP1B expression levels in senescent chondrocytes. Furthermore, *in vitro* tests confirmed that PTP1B knockdown slowed cartilage degradation and prevented chondrocyte senescence in OA. In conclusion, we showed that PTP1B knockdown prevented the senescence of chondrocytes and prevented cartilage degradation in OA. These findings offer a fresh perspective on the pathophysiology of OA, opening up new avenues for OA clinical diagnosis and targeted treatment.

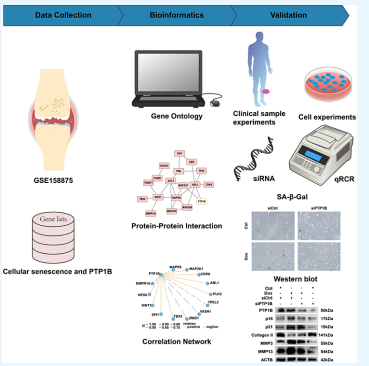

INTRODUCTION

Osteoarthritis (OA), the most common kind of arthritis, is characterized by abnormal growth of osteophytes, synovial inflammation, and a progressive loss of cartilage matrix. More than 67 million people are expected to have OA by 2030, and treatment costs are projected to surpass $3 billion annually. Consequently, OA is a significant health and economic burden.[1−8] The current standard of care for OA consists of pain management and eventually complete joint replacement; the former just deals with symptoms and enhances joint function, while the latter is connected to infection and other comorbidities. However, because of a lack of effective disease-modifying medications, the onset of OA cannot be stopped or suppressed.[9]

The pathogenesis of OA is often connected to aging and aberrant mechanical stress-induced changes in the chondrocyte microenvironment.[10] As cellular senescence is a crucial aspect of aging, chondrocytes exhibit a number of characteristics of senescent cells as we age and the progression of OA.[11,12] Senescent cells are distinguished by their inability to divide, resistance to apoptosis, and strong secretome of the senescence-associated secretory phenotype (SASP), which may change the structure and functionality of the cells and tissues around them. A characteristic of SASP that coincides with mediators involved in the progression of OA is increased production of proinflammatory mediators, such as interleukin (IL)-1, IL-6, and matrix metalloproteinase (MMP)3.[13,14] The molecular processes governing the control of cellular senescence in OA are still unknown as of this writing.

In human chondrocytes, insulin-like growth factor 1 (IGF1) signaling is disrupted with aging, which lowers the expression of extracellular matrix genes and decreases protein synthesis.[15,16] This effect was linked to a higher sensitivity to oxidative stress in human chondrocytes from older adults, which inhibited IGF1-mediated RAC serine/threonine protein kinase (AKT) activation and increased catabolic mitogen-activated protein kinase (MAPK) signaling pathways activation.[16,17] Protein tyrosine phosphatase 1B (PTP1B), which dephosphorylates and inactivates IGFR, is one substance that has been shown to inhibit IGFR activity.[18,19] Simultaneously, research has demonstrated that PTP1B was downregulated by SIRT1, which was crucial in enhancing aging-related health.[20] By suppressing PTP1B, resveratrol enhances insulin sensitivity and lengthens the life span of diet-induced obese (DIO)

Received: December 23, 2023
Revised: February 10, 2024
Accepted: May 30, 2024
Published: June 13, 2024

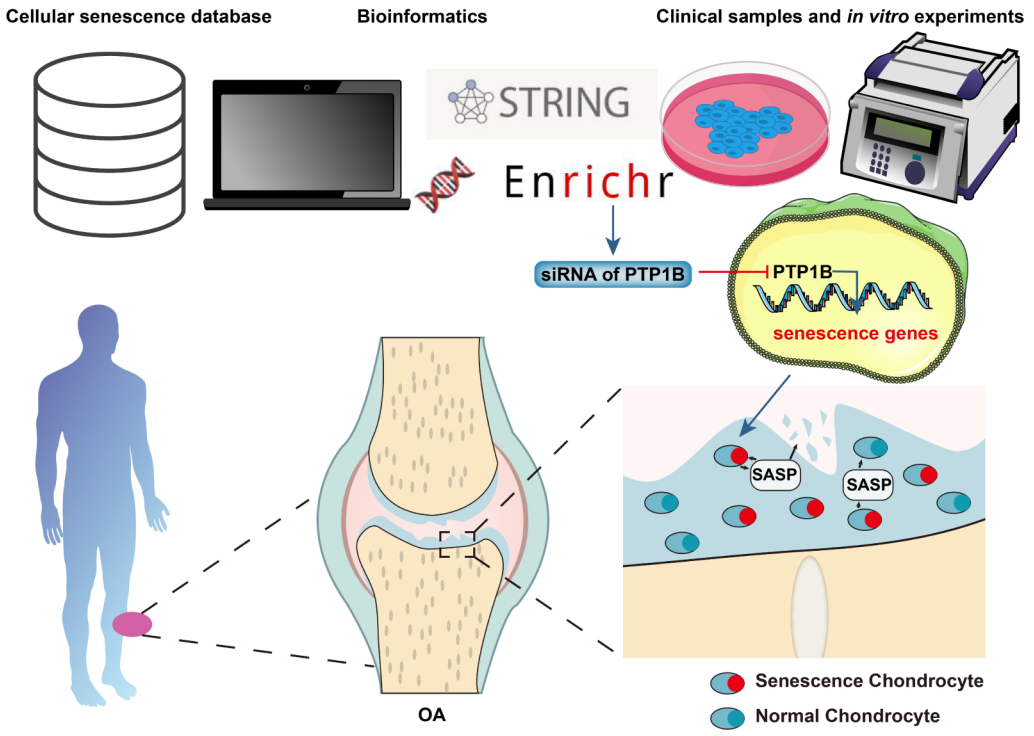

Figure 1. Schematic diagram. We demonstrated that PTP1B knockdown reduced chondrocyte senescence and halted cartilage deterioration in OA using a range of well-established bioinformatics tools, clinical samples, and *in vitro* experimental procedures.

mice.[21−23] These results support the hypothesis that PTP1B represents a suitable target for the treatment of aging and obesity. PTP1B's involvement in chondrocyte senescence and cartilage aging, however, is uncertain, and there is no known molecular relationship between the two.

Through the use of a variety of well-established bioinformatics methodologies, clinical samples, and *in vitro* experimental techniques, we for the first time established the following items in this work: (1) the cellular senescence-related genes implicated in the pathogenesis of OA, their primary biological functions, and likely hub cellular senescence-related genes; (2) the expression of PTP1B in OA and its potential association with cellular senescence; and (3) the effect of PTP1B knockdown.

MATERIALS AND METHODS

The flowchart of this research is shown in Figure 1.

Acquisition and Preprocessing of Data Sets. The Gene Expression Omnibus (GEO) data source (https://www.ncbi.nlm.nih.gov/geo/) was used to retrieve the gene expression profile of OA. Chondrocytes were harvested, and total RNA was extracted using the TRIzol reagent (Takara Bio) after they had been treated with inflammatory cytokines (10 ng/mL IL-1) for 4 h. A total of ~2 × 10^5 cells were employed for the transcriptome analysis of each human chondrocyte sample. Ultimately, the GSE158875 mRNA expression data set was chosen and downloaded for additional investigation. Four samples of human OA chondrocytes and four samples of normal chondrocytes' RNA sequencing data were used to create the expression files for this data set. The expression matrix's "probe id" was changed to "symbol" using a platform annotation file. We determined the average result for several probes corresponding to a single gene symbol as the gene's expression level.

PTP1B Expression Research in GSE158875. To perform a differential analysis, genes having expression levels greater than 0 in at least 90% of the samples from GSE158875 were first chosen. The "sva" R package was used to fix the batch effect caused by the various platforms. To find differentially expressed genes (DEGs), we next utilized DEseq2. The select criteria of DEGs were set as $p < 0.05$ and fold change >1.5.[24−27] To show how these genes differed between samples, we created a gene expression heatmap. Using the R "ggplot2" software, we then produced a DEG volcano plot. The "Violinplot" function of the R programming language was then used to display the variations in PTP1B percentage between samples.[28]

Identification of Genes Associated with OA and Cellular Senescence. Genes associated with cellular senescence were taken from the Gene Set GOBP CELLULAR SENESCENCE in the Molecular Signatures database (http://www.gsea-msigdb.org/gsea/msigdb/index.jsp).[29−31] The related genes for cellular senescence and OA were obtained by intersecting the genes linked to both conditions using a Venn diagram.

Analysis of Functional Enrichment. Gene ontology (GO) study was carried out to understand the biological mechanism, cellular components, and molecular functions of cellular senescence-related DEGs. The signaling pathways connected to the cellular senescence-related DEGs were examined by using Reactome pathway analysis. The GO and Reactome pathway studies were performed on the Enrichr database, and specific findings of the GO and Reactome pathway analyses with $p < 0.05$ were chosen for additional visualization.[32,33]

Analysis of the Relationships Between DEGs Linked to Cellular Senescence. In order to look into potential connections between cellular senescence-related DEGs in OA,

https://doi.org/10.1021/acsomega.3c10313
ACS Omega 2024, 9, 27017−27029

Table 1. Primers Used for qPCR

	primers sequence(5′-3′)	
gene	forward	reverse
ACTB	CAGATGTGGATCAGCAAGCAGGAG	CGCAACTAAGTCATAGTCCGCCTAG
COL2A1	TGAGGGCGCGGTAGAGACCC	TGCACACAGCTGCCAGCCTC
ACAN	CATTCACCAGTGAGGACCTCGT	TCACACTGCTCATAGCCTGCTTC
PTP1B	GCTGATACCTGCCTCTTGCTGATG	ATCCTCCTGGGTCTCTTCCTTCAC
CDKN1A	GATGGAACTTCGACTTTGTCAC	GTCCACATGGTCTTCCTCTG
CDKN2A	GGCACCAGAGGCAGTAACCATG	AGTTGTGGCCCTGTAGGACCTTC
MAP2K1	CAAGCCCTCCAACATCCTAGTCAAC	ATACCTCCCAACCGCCATCTCTAC
ABL1	GCTTCTTGGTGCGTGAGAGTGAG	CTGGATAATGGAGCGTGGTGATGAG
IL1A	CTATCATGTAAGCTATGGCCCA	GCTTAAACTCAACCGTCTCTTC
IL1B	GCCAGTGAAATGATGGCTTATT	AGGAGCACTTCATCTGTTTAGG
IL6	CACTGGTCTTTTGGAGTTTGAG	GGACTTTTGTACTCATCTGCAC
IL8	AACTGAGAGTGATTGAGAGTGG	ATGAATTCTCAGCCCTCTTCAA
IL13	CATGTCCGAGACACCAAAATC	CCCTCGCGAAAAAGTTTCTTTA
MMP3	GGCAAGACAGCAAGGCATAGAGAC	ACGCACAGCAACAGTAGGATTGG
MMP13	CACTTTATGCTTCCTGATGACG	TCTGGCGTTTTTGGATGTTTAG

correlation research across these DEGs was carried out using the Pearson test. Statistical significance was assigned to correlated pairings with $|r| > 0.50$ and $p < 0.05$. A correlation network was also built using couples with $|r| > 0.50$ and $p < 0.05$.

Analysis of the PPI Between PTP1B and DEGs Connected to Cellular Senescence. It was common practice to utilize the STRING database (https://cn.string-db.org) to examine the association networks of functional proteins.[34,35] STRING (version 11.5, https://cn.string-db.org/) was used to create the protein−protein interaction (PPI) network, and a confidence score of >0.4 was used. For visualization, Cytoscape (version 3.9.1) was utilized. For further investigation, all PTP1B and cellular senescence-related DEGs ranked by the PPI score were chosen.

Analysis of the Relationship Between Cellular Senescence and PTP1B. To explore any potential connections between PTP1B and cellular senescence in OA, Pearson test was used to conduct a correlation study between PTP1B and senescence-related DEGs. The regulatory network was constructed by integrating the couples with $|r| > 0.50$ and $p < 0.05$.

Clinical Samples' Experimental Verification. *Cartilage Sample Collection.* Samples of damaged cartilage from patients (n = 3; male: 1, female: 2; mean age: 65 years; range: 60−76 years) who underwent total knee arthroplasty (TKA) surgery due to knee OA were collected. The patients (n = 3; 1 male and 2 female; mean age: 45 years; range: 38−59 years) who underwent lower limb amputation in the hospital for trauma provided normal cartilage samples. The informed consent form was signed before sample collection by each participant, who consented to take part in the scientific study. The Shanxi Medical University's Second Hospital';s ethical committees gave their approval for the sample collection and the research protocol.

Histological Evaluation. Human cartilage samples were decalcified for 8 weeks in a 10% solution of ethylenediaminetetraacetic acid (pH 7.2) after being fixed in 4% buffered paraformaldehyde for 48 h. Following standard tissue preparation, these samples were embedded in paraffin, and coronal slices measuring 6-m thick were produced using a rotary microtome (Leica Microsystems GmbH).

The sections were stained with Safranin O/Fast Green (Sigma-Aldrich; Merck KGaA) after deparaffinization in xylene, rehydration in graded ethanol solutions, and finally in H_2O.

Immunohistochemistry. These human tissue samples were cut into paraffin-embedded slices, which were then immunostained for the expression of PTP1B and p21. For 10 min at room temperature, the deparaffinized and rehydrated sections were treated in 3% H2O2 in phosphate-buffered saline (PBS) to inhibit any endogenous peroxidase activity. To reveal antigens that could have been obscured by tissue fixation and processing, the sections were first cleaned with PBS before being digested with 0.1% trypsin at 37 °C for 30 min. The sections were then treated with 20% normal serum for 30 min at room temperature, followed by overnight incubation at 4 °C with antihuman PTP1B (1:100; cat. no. sc-6246; Santa Cruz Biotechnology) and antihuman p21 (1:100; cat. no. 11334-1-AP; Proteintech). The slices were then briefly treated in 3,3′-diaminobenzidine solution before being rinsed three times with PBS and incubated at 37 °C for 30 min with a secondary antibody (ZSGB-BIO) coupled to horseradish peroxidase. For quantification, the immunostained sections were examined and captured on a camera by using a Leica DM6B microscope (Leica Microsystems GmbH).

***In Vitro* Experimental Verification.** *Cell Culture.* The immortalized human chondrocyte cell line C28/I2 was created in the lab of Professor Mary B. Goldring (Hospital for Special Surgery/Weill Medical College of Cornell University, New York, NY). It was isolated from the costal cartilage of a 15-year-old female and immortalized using SV-40 large T-antigen.[36] C28/I2 cells were cultured in DMEM/high glucose medium with 10% FBS added. The cells were divided in a new medium after being isolated using the trypsin-EDTA (Gibco) solution, after they had achieved around 90% confluence. To induce senescence in C28/I2 cells, 7 days of exposure to 100 ng/mL doxorubicin (Dox, SC0159, Beyotime, China) was required.[37] The dox-containing medium was replaced every 2 days.

Transfection and Treatment. Chondrocytes were transfected for 48 h with either the PTP1B siRNA (GenePharma, Shanghai, China) or the negative control siRNA using the Lipofectamine RNAiMAX Reagent from Invitrogen in Carlsbad, California. To mimic the cellular senescence

https://doi.org/10.1021/acsomega.3c10313
ACS Omega 2024, 9, 27017−27029

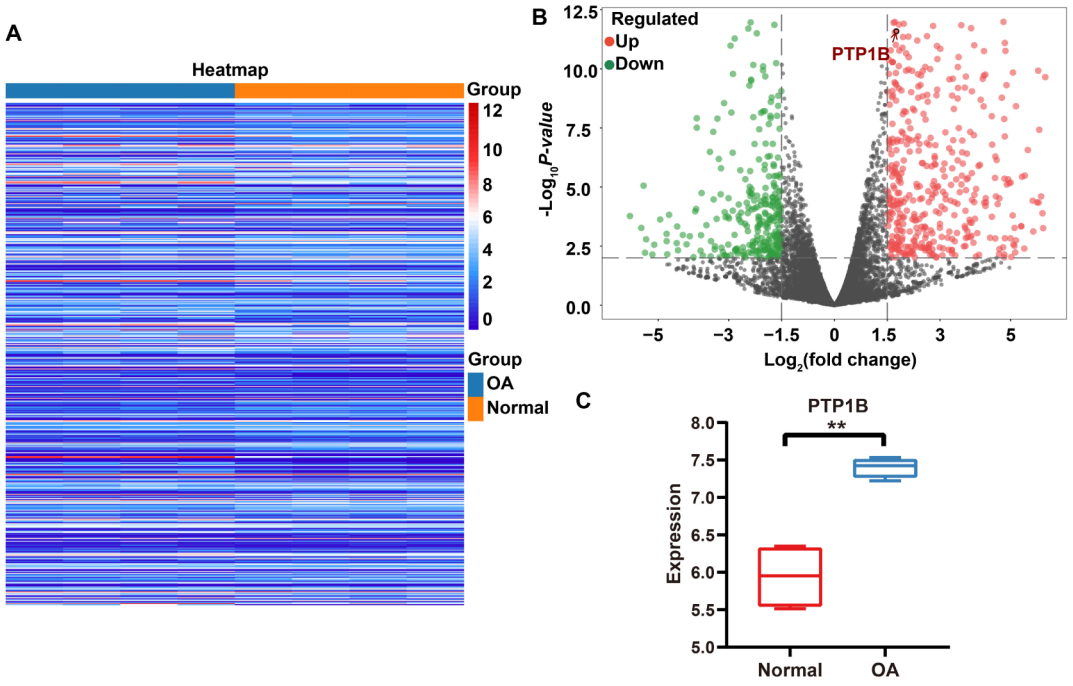

Figure 2. Identification of PTP1B in GEO. Heatmap of gene expression for OA and normal samples are shown in (A), volcano plots of OA-related genes are shown in (B), and PTP1B's differential mRNA expression in OA and normal samples is shown in (C). The red and green dots, meanwhile, stand for the upregulated and downregulated RNAs, respectively. The black dots indicate RNAs that are not differentially expressed, $^{**}p < 0.01$.

environment of osteoarthritis, chondrocytes were treated with 100 ng/mL dox (SC0159, Beyotime, China) for an additional 24 h after transfection. The sequences of negative control siRNA (siCtrl) or PTP1B siRNA (siPTP1B) were: siCtrl, sense 5′-UUCUCCGAACGUGUCACGUTT-3′, antisense 5′-ACGUGACACGUUCGGAGAATT-3′; and siPTP1B, sense 5′-GAGCCACACAAUGGGAAAUTT-3′, antisense 5′-AUUUCCCAUUGUGUGGCUCTT-3′.

Western Blot Analysis. Cells were processed to extract their total protein content, and BCA tests (Beyotime) were used to calculate the protein concentration. The proteins were separated by SDS-polyacrylamide gel electrophoresis and then transferred to a polyvinylidene difluoride membrane. The membrane was incubated with the primary antibody overnight at 4 °C after being blocked with 5% BSA for 1 h at room temperature. Antirabbit and antimouse IgG (1:3000, Thermo Fisher Scientific, USA) were then incubated on the membrane for 120 min. Then, immunolabeled bands were seen using an enhanced chemiluminescence reagent from Thermo Fisher Scientific in the United States. The level of protein expression was calculated using ImageJ. The antibodies used for Western blotting were anti-PTP1B (1:2000, Santa Cruz Biotechnology), anti-p16 (1:1000, Abcam), anti-p21 (1:2000, Santa Cruz Biotechnology), anti-ACTB (1:2000, Proteintech), anti-Collagen II (1:2000, Proteintech), anti-MMP3 (1:1000, Proteintech), and anti-MMP13 (1:500, Proteintech).

Quantitative Real-Time PCR. Total RNA was extracted from cells or tissues using the TRIzol reagent (Invitrogen) in accordance with the manufacturer's instructions. The cDNA was created by using HiScript Q RT SuperMix (Vazyme, Nanjing, China). The ABI Step-One Plus Real-Time PCR System and ChamQ SYBR qPCR Master Mix (Vazyme) (Applied Biosystems) were used to perform qPCR. The findings were normalized using ACTB as an internal check after the data were processed using the $2^{-\Delta\Delta Ct}$ method. All primers were listed in Table 1.

SA-β-Gal Staining. Senescence-associated -galactosidase (SA-β-Gal) staining was done using a Beyotime Biotechnology cell senescence β-galactosidase staining kit and adhering to the manufacturer's instructions. Cells were briefly washed in PBS before being fixed for 5 min in 2% PFA and 0.2% glutaraldehyde. After cleaning, the cells were allowed to soak in the SA-β-Gal staining solution for 16 h at 37 °C. After incubation, the cells were cleaned, and a Nikon Eclipse Ni−U 131 microscope was used to take pictures of them. Three random locations per culture dish were counted for total cells and SA-β-Gal-positive cells by using ImageJ.

Statistical Analysis. In our investigation, R (version 4.4.1) was employed. Pearson analysis was used for correlation analysis, and the "pheatmap" R package was used to generate heatmaps. Graph prism software (version 5.0; Graph Prism Software, Inc.) and SPSS software (version 19.0; IBM Corporation) are used to statistically evaluate the data, which are reported as the mean SEM. To determine if the data were normally distributed, the Shapiro−Wilk test was applied. For values having a normal distribution, unpaired Student's *t* tests across two groups and one-way analysis of variance across multiple groups were utilized. The Mann−Whitney test (2 groups) and the Kruskal−Wallis test (multiple groups) were used for values with non-normal distribution. *p* values were considered significant at $^{*}p < 0.05$, $^{**}p < 0.01$, and $^{***}p < 0.001$.

RESULTS

Determination of DEGs. With the criteria of fold change >1.5 and $p < 0.05$, a total of 2717 DEGs were found, as indicated in the heatmap and volcano plot (Supporting Table 1

https://doi.org/10.1021/acsomega.3c10313
ACS Omega 2024, 9, 27017−27029

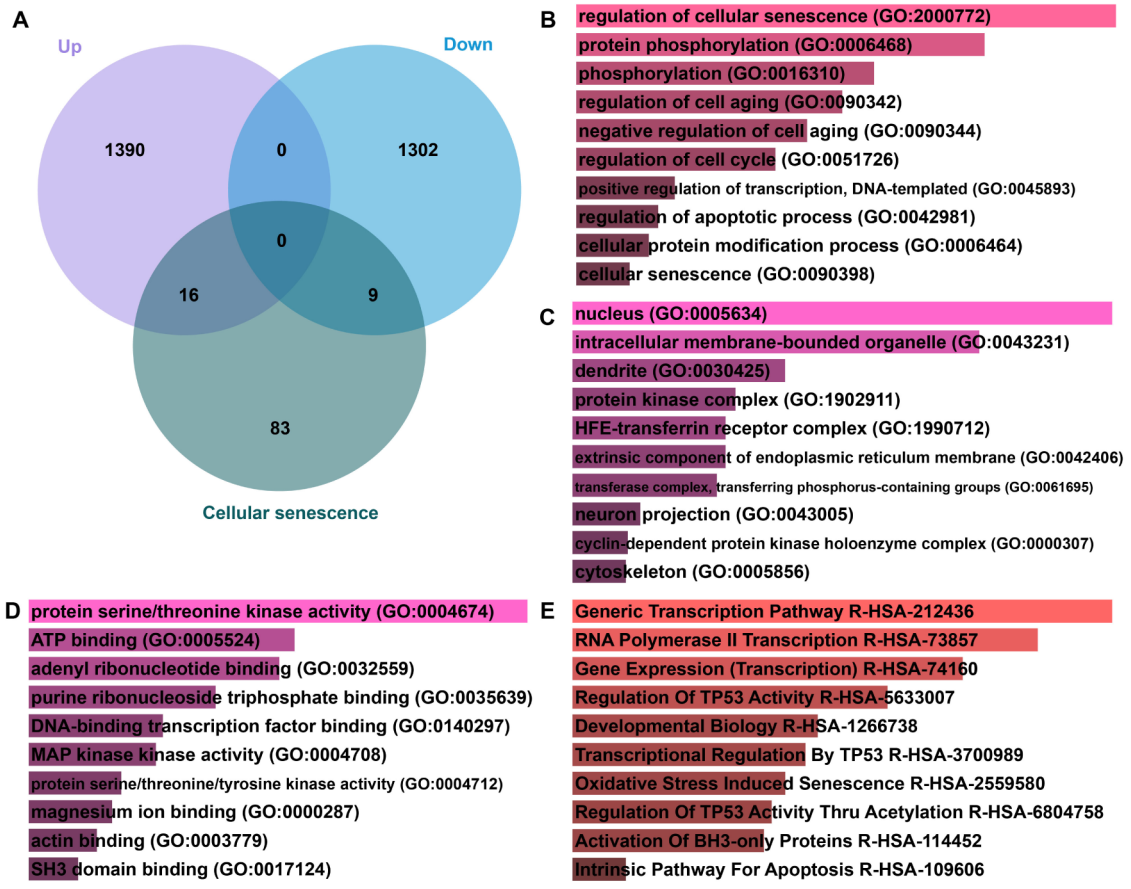

Figure 3. Cellular senescence-related DEG identification and function analysis. (A) Genetic overlap with genes associated with OA and cellular senescence. For the DEGs connected to cellular senescence, GO (biological process, cell component, and molecular function) and pathway annotation were used. (B) biological process; (C) cell component; (D) molecular function; (E) pathway. Ranking by-log10(*p*-value).

Table 2. Top 10 Items in the Biological Process

term	overlap	p-value	adjusted p-value	odds ratio	combined Score
regulation of cellular senescence (GO:2000772)	8/31	1.32×10^{-17}	9.00×10^{-15}	408.2250639	15865.72523
protein phosphorylation (GO:0006468)	13/496	4.55×10^{-15}	1.55×10^{-12}	43.71911663	1443.739696
phosphorylation (GO:0016310)	11/400	6.19×10^{-13}	1.41×10^{-10}	39.56041131	1112.058579
regulation of cell aging (GO:0090342)	5/13	2.55×10^{-12}	4.34×10^{-10}	623.96875	16657.402
negative regulation of cell aging (GO:0090344)	5/17	1.22×10^{-11}	1.66×10^{-09}	415.8958333	10451.00104
regulation of cell cycle (GO:0051726)	9/296	5.01×10^{-11}	5.68×10^{-09}	38.58710801	915.1878218
positive regulation of transcription, DNA-templated (GO:0045893)	12/1183	4.40×10^{-09}	4.28×10^{-07}	14.82283387	285.2233903
regulation of apoptotic process (GO:0042981)	10/742	9.17×10^{-09}	7.81×10^{-07}	17.52550091	324.3485141
cellular protein modification process (GO:0006464)	11/1025	1.39×10^{-08}	1.06×10^{-06}	14.69223725	265.7516199
cellular senescence (GO:0090398)	4/27	3.27×10^{-08}	2.22×10^{-06}	165.2339545	2848.112932

Table 3. Top 10 Items in the Cell Component

term	overlap	p-value	adjusted p-value	odds ratio	combined score
nucleus (GO:0005634)	15/4484	5.62×10^{-05}	0.002248326	5.204520027	50.93376961
intracellular membrane-bounded organelle (GO:0043231)	15/5192	3.33×10^{-04}	0.0066616	4.287618312	34.33150782
dendrite (GO:0030425)	3/270	0.004492014	0.059893522	10.06537283	54.40791072
protein kinase complex (GO:1902911)	1/7	0.008718464	0.063977326	138.6736111	657.633561
HFE-transferrin receptor complex (GO:1990712)	1/8	0.009957992	0.063977326	118.8571429	547.857721
extrinsic component of endoplasmic reticulum membrane (GO:0042406)	1/8	0.009957992	0.063977326	118.8571429	547.857721
transferase complex, transferring phosphorus-containing groups (GO:0061695)	1/9	0.011196032	0.063977326	103.9947917	467.164971
neuron projection (GO:0043005)	3/556	0.031213306	0.151430473	4.789248726	16.60389819
cyclin-dependent protein kinase holoenzyme complex (GO:0000307)	1/30	0.036854213	0.151430473	28.65804598	94.59405782
cytoskeleton (GO:0005856)	3/600	0.037857618	0.151430473	4.426222019	14.49111026

https://doi.org/10.1021/acsomega.3c10313
ACS Omega 2024, 9, 27017−27029

Table 4. Top 10 Items in Molecular Function

term	overlap	p-value	adjusted p-value	odds ratio	combined score
protein serine/threonine kinase activity (GO:0004674)	9/344	1.90×10^{-10}	1.66×10^{-08}	32.97761194	738.1248124
ATP binding (GO:0005524)	6/278	9.69×10^{-07}	4.22×10^{-05}	22.875	316.7461954
adenyl ribonucleotide binding (GO:0032559)	6/306	1.69×10^{-06}	4.91×10^{-05}	20.71052632	275.2227003
purine ribonucleoside triphosphate binding (GO:0035639)	6/460	1.75×10^{-05}	3.81×10^{-04}	13.5782518	148.7266903
DNA-binding transcription factor binding (GO:0140297)	4/208	1.21×10^{-04}	0.002107539	18.46031746	166.4881536
MAP kinase kinase activity (GO:0004708)	2/15	1.56×10^{-04}	0.002261128	133.5250836	1170.486231
protein serine/threonine/tyrosine kinase activity (GO:0004712)	2/28	5.56×10^{-04}	0.006908112	66.71906355	500.063177
magnesium ion binding (GO:0000287)	3/146	7.79×10^{-04}	0.008472227	18.91163382	135.3586666
actin binding (GO:0003779)	3/177	0.001358082	0.013128129	15.51802508	102.4450615
SH3 domain binding (GO:0017124)	2/62	0.002709221	0.023570227	28.86231884	170.6078788

Table 5. Top 10 Items in Pathway

term	overlap	p-value	adjusted p-value	odds ratio	combined score
generic transcription pathway R-HSA-212436	11/1190	6.50×10^{-08}	1.44×10^{-05}	12.52611172	207.3008899
RNA polymerase II transcription R-HSA-73857	11/1312	1.76×10^{-07}	1.95×10^{-05}	11.27780828	175.4165955
gene expression (transcription) R-HSA-74160	11/1449	4.79×10^{-07}	3.55×10^{-05}	10.12850189	147.3782851
regulation of TP53 activity R-HSA-5633007	5/157	1.31×10^{-06}	7.26×10^{-05}	32.60361842	441.6663224
developmental biology R-HSA-1266738	9/1073	3.33×10^{-06}	1.45×10^{-04}	9.997591635	126.0891076
transcriptional regulation by TP53 R-HSA-3700989	6/354	3.93×10^{-06}	1.45×10^{-04}	17.81034483	221.6937054
oxidative stress induced senescence R-HSA-2559580	4/93	5.14×10^{-06}	1.63×10^{-04}	42.55965757	518.2948998
regulation of TP53 activity thru acetylation R-HSA-6804758	3/29	6.17×10^{-06}	1.69×10^{-04}	104.6276224	1255.096032
activation of BH3-only proteins R-HSA-114452	3/30	6.85×10^{-06}	1.69×10^{-04}	100.7474747	1198.018615
intrinsic pathway for apoptosis R-HSA-109606	3/55	4.34×10^{-05}	9.63×10^{-04}	52.24562937	524.8593532

and Figure 2A,B). The relative expression of PTP1B in GSE158875 was then found. The findings demonstrated that IL-1β-induced OA chondrocytes had considerably increased PTP1B expression (Figure 2C). We intersected these 2717 DEGs with the Gene Set from the Molecular Signatures database to create 25 DEGs that are specifically associated with cellular senescence (Figure 3A).

GO and KEGG Enrichment Analysis of Cellular Senescence-Related DEGs. The biological roles of DEGs connected to cellular senescence were investigated using GO analysis, which included biological processes, cell components, and molecular functions. These cellular senescence-associated DEGs were mostly abundant in biological processes linked to controlling cellular senescence, protein phosphorylation, phosphorylation, controlling cell aging, and controlling cell aging negatively (Figure 3B and Table 2). The main molecular functions of these cellular senescence-related DEGs were protein serine/threonine kinase activity, ATP binding, and adenyl ribonucleotide binding (Figure 3C,D, Tables 3 and 4). They also elicited the cell component primarily at the nucleus, intracellular membrane-bound organelle, dendrite, and protein kinase complex. These cellular senescence-related DEGs, according to Reactome pathway analysis, were mostly engaged in the biological processes of general transcription pathway, oxidative stress-induced senescence, and regulation of Tp53 activity through acetylation (Figure 3E and Table 5).

Correlation Analysis Among Cellular Senescence-Related DEGs. The heat map (Figure 4A) displayed the expression of these DEGs associated with cellular senescence in chondrocytes from healthy cells and OA-induced by IL-1β conditions. The correlation analysis among cellular senescence-related DEGs was conducted (Figure 4B), and the correlation network was also constructed based on $|r| > 0.50$ and $p < 0.05$ (Figure 4C). The couples with $|r| > 0.95$ and $p < 0.05$ were depicted in Figure 4D−I. ABL1-MAP2K1 pair was the most positively correlated pair ($r = 0.93$, $p < 0.01$), and PLK2-BMPR1A pair was the most negatively correlated pair ($r = -0.90$, $p < 0.01$) among the DEGs related to cellular senescence.

PPI Analysis and Correlation Analysis Between PTP1B and Cellular Senescence-Related DEGs. In addition to conducting the correlation analysis between PTP1B and the DEGs linked to cellular senescence, the correlation network was also built (Figure 5A). A network of 26 nodes and 24 edges was used for the PPI analysis of PTP1B and DEGs linked to cellular senescence (PPI enrichment $p < 0.01$) (Figure 5B). Combining the PPI analysis and correlation analysis, it is possible that PTP1B is more closely connected to DEGs associated with cellular senescence, such as ABL1 and MAP2K1 (Figure 5C−F).

OA Development is Highly Correlated with Cartilage Senescence and PTP1B Overexpression. We started by gathering cartilage samples from six individuals who had surgery and separating them into OA cartilage tissues and comparable nonlesion samples. In contrast to the injured region, which was fractured, the tissue was rather smooth when stained with safranin O and quickly green (Figure 6A). The qPCR revealed that the normal samples expressed higher levels of COL2A1, and ACAN, whereas they exhibited lower levels of MMP-13, compared to those of the OA group (Figure 6B). In addition, we initially looked at the expression of p21, a characteristic biomarker of senescent cells, in human OA cartilage tissues in order to investigate the involvement of cellular senescence in the development of OA. In the cartilage of OA patients, the protein level of p21 was markedly increased (Figure 6C). The qPCR revealed that the normal samples exhibited lower levels of mRNA expression of p16 and p21, compared with those of the OA group (Figure 6D). Besides, we initially used dox to cause the cellular senescence of chondrocytes for 7 days. According to SA-β-Gal staining,

https://doi.org/10.1021/acsomega.3c10313
ACS Omega 2024, 9, 27017−27029

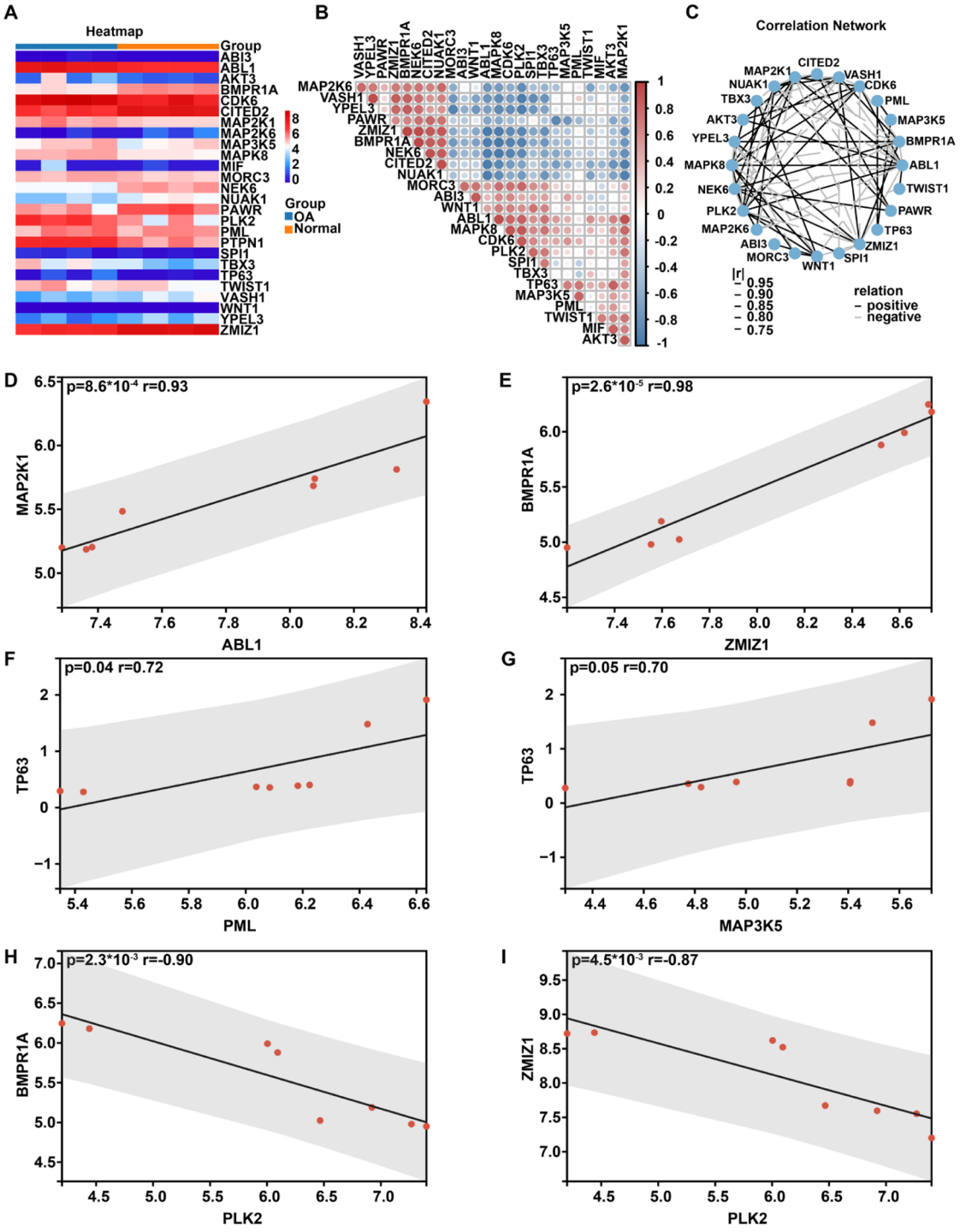

Figure 4. DEGs associated with cellular senescence were correlated. (A) Heat map comparing the expression of DEGs related to cellular senescence in OA and normal samples; (B) correlation heatmap of DEGs related to cellular senescence; (C) correlation network of DEGs related to cellular senescence; (D) Correlation analysis between ABL1 and MAP2K1; (E) correlation analysis between ZMIZ1 and BMPR1A; (F) correlation analysis between PML and TP63; (G) correlation analysis between MAP3K5 and TP63; (H) correlation analysis between PLK2 and BMPR1A; and (I) correlation analysis between PLK2 and ZMIZ1.

Western blot, and qPCR, we saw an accumulation and phenotypical characterization of senescent chondrocytes in the dox group as well as higher expression levels of p16, p21, and SA-β-Gal (Figure 6E,F,J). Further evidence of the excessive chondrocyte senescence brought on by dox was provided by increased SASP mRNA and protein levels (Figure 6G,J). Then, the expression of PTP1B was then analyzed in 3 pairs of OA cartilage tissues and matched nonlesion samples. Immunohistochemical staining was used to assess the expression of the PTP1B protein (Figure 6H). The findings demonstrated that OA cartilage had considerably greater PTP1B expression than nonlesion tissues. In addition, the mRNA and protein expression of PTP1B were higher in senescence chondrocyte (Figure 6I,J).

Expression of PTP1B and Cellular Senescence-Related DEGs. Senescent chondrocytes had considerably

https://doi.org/10.1021/acsomega.3c10313
ACS Omega 2024, 9, 27017−27029

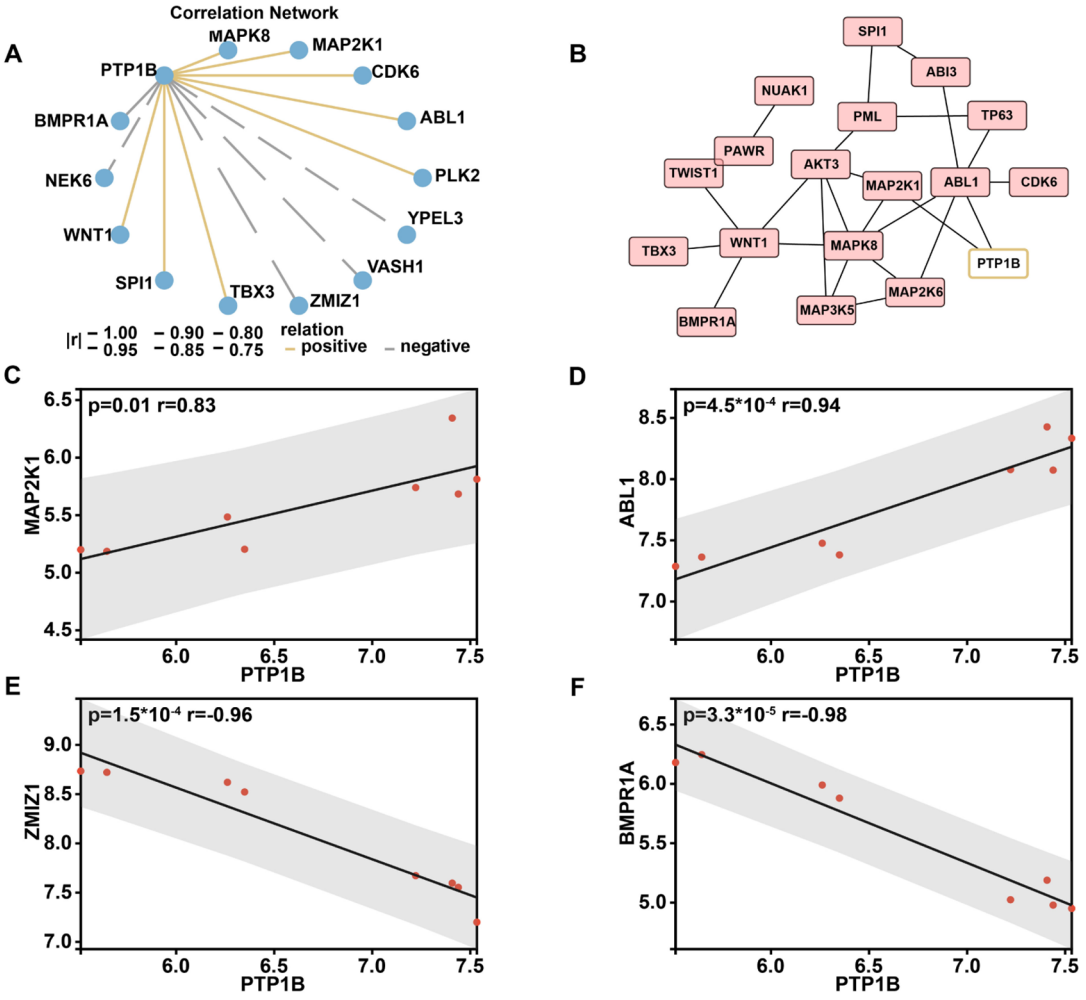

Figure 5. PPI network and correlation study of DEGs and PTP1B connected to cellular senescence. (A) The PTP1B and cellular senescence-related DEGs correlation network; (B) the PTP1B and cellular senescence-related DEGs PPI network; (C) the PTP1B and ABL1 correlation analysis; (D) the PTP1B and MAP2K1 correlation analysis; (E) the PTP1B and ZMIZ1 correlation analysis; (F) the PTP1B and BMPR1A correlation analysis.

higher levels of mRNA for cellular senescence-related DEGs such as MAP2K1 and ABL1 compared to the control group (Figure 7A). Besides, the findings of the correlation analysis demonstrated a positive association between PTP1B and ABL1 and MAP2K1 (r = 0.95, p < 0.01; and r = 0.89, p < 0.01, respectively) (Figure 7B). Furthermore, the findings of the correlation analysis demonstrated a positive association between PTP1B and CDKN1A and CDKN2A (r = 0.79, p < 0.01; and r = 0.78, p < 0.01, respectively) (Figure 7C).

Effects of PTP1B Knockdown on Chondrocyte Senescence. Using PTP1B siRNA, we inhibited chondrocyte senescence to establish that PTP1B governs senescence. By inhibiting PTP1B, we also saw a reduction in the accumulation and morphological characteristics of senescent chondrocytes, as shown by SA-β-Gal staining (Figure 8A). Besides, PTP1B knockdown could suppress the expression of p16, p21, and SASP, while contributing to the expression of collagen II (Figure 8B–E).

DISCUSSION

The destruction of periarticular bone and cartilage is a significant contributing element to OA, a prevalent chronic joint degenerative disease.[38] It has been demonstrated that cellular senescence happens in OA chondrocytes and accelerates the development of OA.[39,40] Therefore, it is crucial to understand how cellular senescence-related genes in chondrocytes work in order to treat OA. Candidate biomarkers associated with cellular senescence can be found using bioinformatics techniques. Bioinformatics has been effectively employed in several prior studies to pinpoint prospective osteoarthritis target genes. In the aged meniscus, the LTF expression was shown to be higher. By activation of the NF-B signaling pathway, LTF might cause meniscal senescence and degeneration. These findings suggested that LTF may serve as a possible treatment target for meniscal degeneration associated with aging as well as a diagnostic marker.[41] In primary chondrocytes, DPP-4 expression was linked to increased senescence-related β-galactosidase activity, p16 expression, senescence-related gene and catabolic gene expression (ADAMTS5, MMP13, IL6, and IL8), increased senescence-associated secretory phenotype secretion, and decreased anabolic gene expression (COL2A1 and ACAN).[42] In this study, 25 hub cellular senescence-related DEGs were selected, their important biological roles were described, and correlation networks were built by using a variety of bioinformatic techniques.

https://doi.org/10.1021/acsomega.3c10313
ACS Omega 2024, 9, 27017−27029

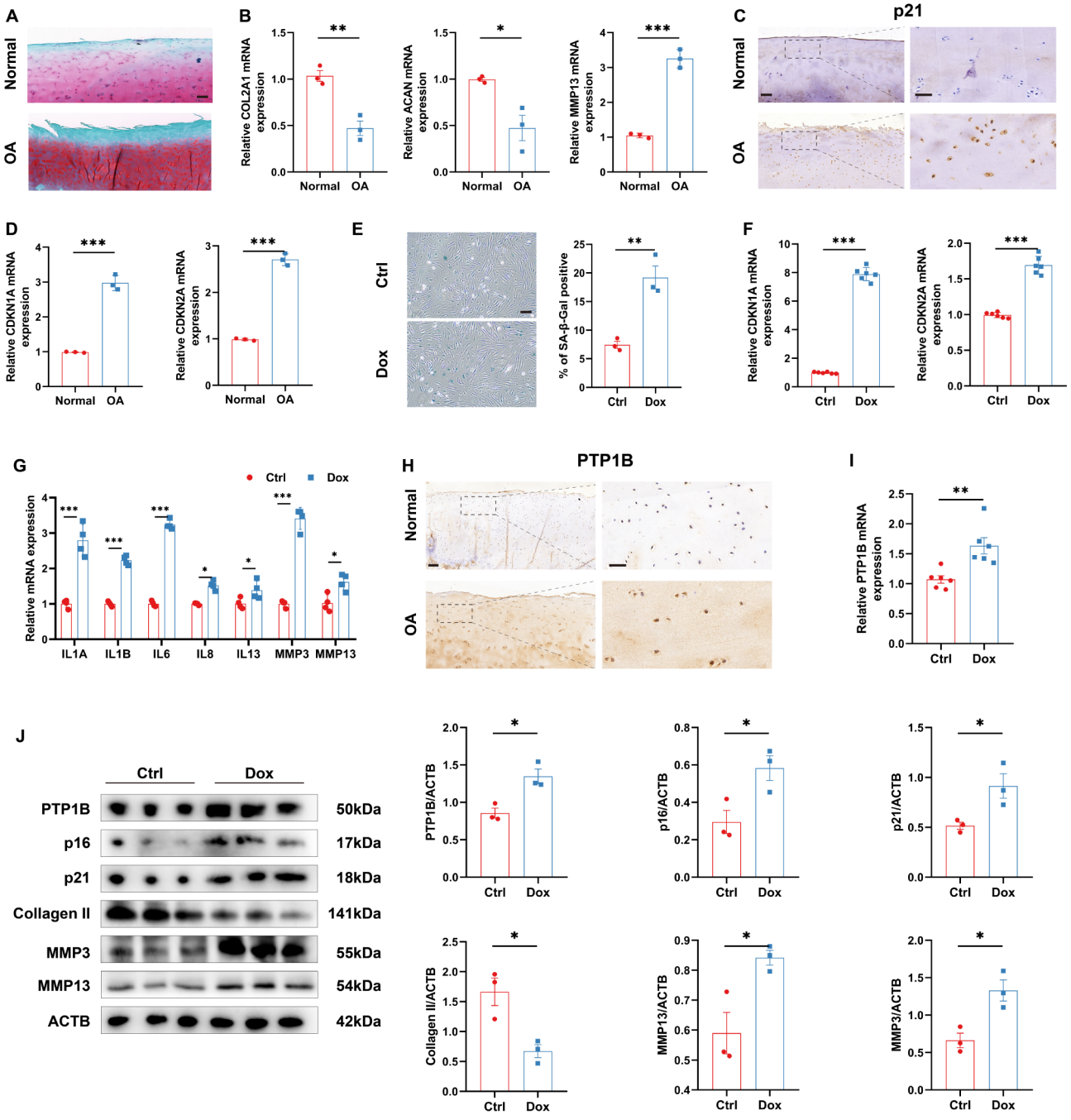

Figure 6. PTP1B expression is elevated in OA cartilage along with cellular senescence associated with OA etiology. Representative images of healthy and OA cartilage tissues are shown in (A), scale bar, 200 μm; (B) COL2A1, ACAN, and MMP13 mRNA expression was analyzed by qPCR; anti-p21 immunohistochemistry assay in healthy and OA cartilage tissues (C), scale bar, left, 200 μm; right, 50 μm (D) CDKN1A, and CDKN2A mRNA expression was analyzed by qPCR; (E) representative photos of SA-β-Gal-stained C28/I2 cells from the control and dox groups, along with a quantitative analysis of SA-β-Gal-stained C28/I2 cells. n = 3, scale bar, 200 μm; (F) qPCR analysis of mRNA levels of CDKN1A, and CDKN2A in C28/I2 cells, n = 6; (G) qPCR analysis of mRNA levels of SASP-related inflammatory cytokines (IL-1α, IL-1β, IL-6, IL-8, and IL-13), MMP3 and MMP13 in C28/I2 cells, n = 4; anti-PTP1B immunohistochemistry test in healthy and OA cartilage tissues (H), scale bar, left, 200 μm; right, 50 μm; (I) qPCR analysis of mRNA levels of PTP1B in C28/I2 cells, n = 6; (J) representative Western blot and quantification of PTP1B, p16, p21, Collagen II, MMP3, and MMP13 in C28/I2 cells, n = 3, *p < 0.05, **p < 0.01, ***p < 0.001; all data were presented as the means ± SEM. Student's t test was used for statistical analysis.

PTP1B, SHP1, SHP2, and LAR are among the phosphatases that make up the protein tyrosine phosphatase (PTP) family and function to inhibit tyrosine kinase activity.[21,43,44] PTP1B has been demonstrated to serve as an essential insulin receptor phosphatase and a negative regulator of the insulin signal transduction cascade.[45,46] In comparison to wild-type mice, PTP1B-deficient animals are more insulin-sensitive, have better glycemic control, and are more resistant to diet-induced obesity.[47] Previous research has shown that human chondrocytes' IGF1 signaling is disrupted with aging, which lowers the expression of extracellular matrix genes and protein production.[16,48] Earlier work showed that SirT1-mediated

https://doi.org/10.1021/acsomega.3c10313
ACS Omega 2024, 9, 27017−27029

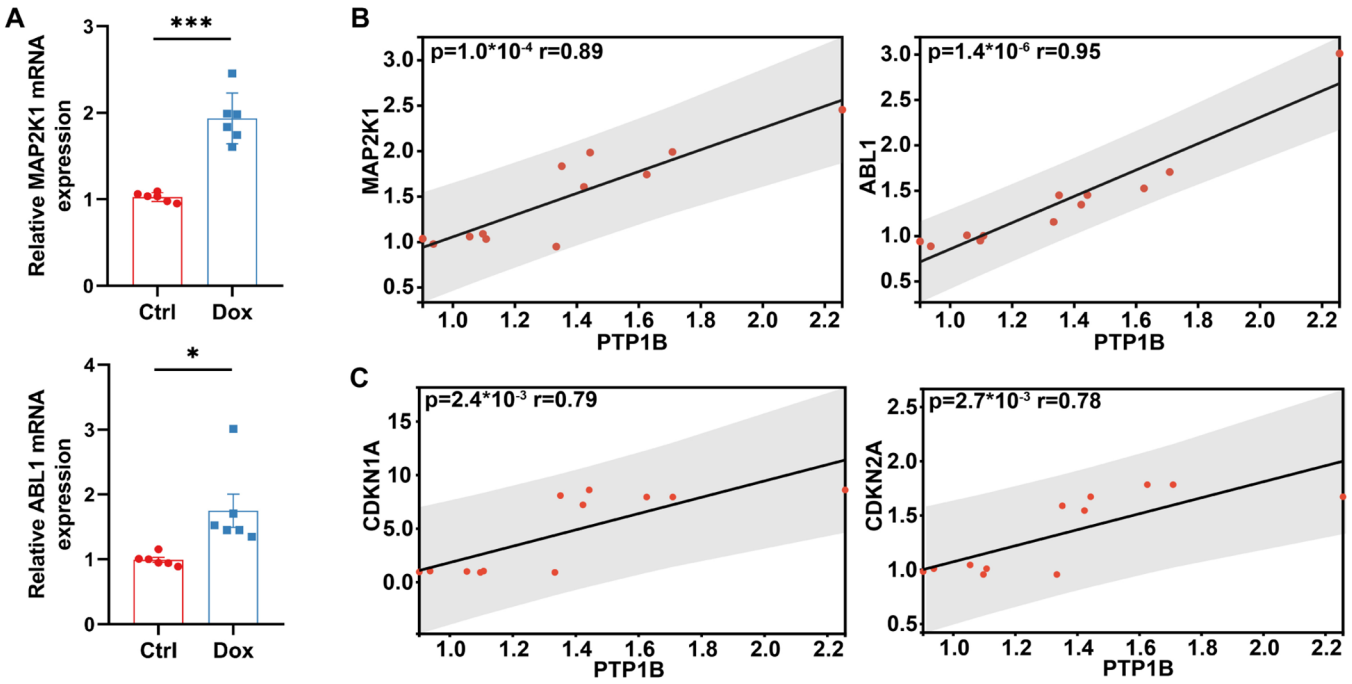

Figure 7. Senescent chondrocytes have increased PTP1B expression that is positively connected with genes associated with cellular senescence. (A) qPCR analysis of mRNA levels of PTP1B in C28/I2 cells, $n = 6$, $^{*}p < 0.05$, $^{***}p < 0.001$; (B) correlation analysis of mRNA levels of PTP1B with ABL1 and MAP2K1 in C28/I2 cells. (C) correlation analysis of mRNA levels of PTP1B with CDKN1A and CDKN2A in C28/I2 cells. All data were presented as the means ± SEM. Student's *t* test was used for statistical analysis.

suppression of PTP1B contributed to the activation of IGFR, at least in part. While siRNA-mediated downregulation of PTP1B greatly reduced apoptosis, overexpression of PTP1B in chondrocytes enhanced apoptosis and lowered IGFR phosphorylation. PTP1B levels are increased in OA cartilage when SirT1 levels are lowered, according to research on normal donors and OA patients' cartilage.[22,49] Recent research by Zhu et al. indicates PTP1B is a key regulator of cellular aging since PTP1B knockdown extends longevity in yeast and human cells.[50] PTP1B's involvement in chondrocyte senescence and cartilage aging, however, is uncertain, and there is no known molecular relationship between the two. The findings of our study's clinical samples and *in vitro* tests revealed that the expression of PTP1B matched those of our bioinformatics analysis of GSE158875. The strong correlation observed in our study suggests that PTP1B and cellular senescence may be related to the pathomechanism of OA. We first used the correlation network analysis to identify 25 hub cellular senescence-related DEGs, and then we used the Pearson analysis to try to understand how they relate to other cellular senescence-related DEGs. It is fascinating that PTP1B and the bulk of DEGs linked to cellular senescence exhibited a substantial relationship since it shows a connection between the two in OA. Combining the PPI analysis and correlation analysis, PTP1B may be more closely connected to DEGs associated with cellular senescence, such as MAP2K1 and ABL1, according to the findings of our *in vitro* tests. The findings presented above seem to confirm our theory that PTP1B deficiency or inhibition may slow the course of OA by preventing chondrocyte senescence.

To verify the aforementioned theory, we looked at how the expression of PTP1B and p21 varied between OA and non-OA cartilage tissues. Without a doubt, we discovered that OA dramatically upregulated the expression of PTP1B and p21. PTP1B knockdown was demonstrated to prevent OA-related cartilage degradation *in vitro* studies through the increased expression of Collagen II and reduced expression of SASP, which includes IL-1, IL-6, and MMP3. Additionally, its reduction prevented chondrocyte senescence, as seen by the lowered SA-β-Gal, p21, and p16 expression levels. Further research is necessary, nevertheless, to fully understand the intricate process by which PTP1B controls chondrocyte senescence to control cartilage deterioration. Tyrosine-protein kinase Abl1 was shown to be an NSC aging factor by a single-cell transcriptome study of quiescence in deep neural stem cells (NSCs), which also showed multiple markers of molecular aging in the mature brain. In the middle-aged brain, treatment with the Abl inhibitor imatinib enhanced NSC activation without compromising NSC maintenance.[51] Ras is initially mitogenic in primary cells but later triggers premature senescence involving tumor suppressors p53 and p16. Inducing both p53 and p16, constitutive activation of MEK (a part of the MAPK cascade, such as MAP2K1) is necessary for Ras-induced senescence of normal human fibroblasts.[52] Consequently, the PTP1B and ABL1 interaction may trigger the MAPK signaling pathway and encourage chondrocyte senescence.

There are still certain limitations, even though this study employed bioinformatic methods to collect a ton of important data that were later verified in trials. First of all, while we tried to explain how PTP1B could be related to cellular senescence in OA, the analysis carried out in the current study was fairly brief and needs more investigation. Second, there are not many studies on how cells operate. Last but not least, no additional *in vivo* and *in vitro* experimental studies of the precise processes behind this process have been carried out; these studies will be the focus of future studies.

https://doi.org/10.1021/acsomega.3c10313
ACS Omega 2024, 9, 27017−27029

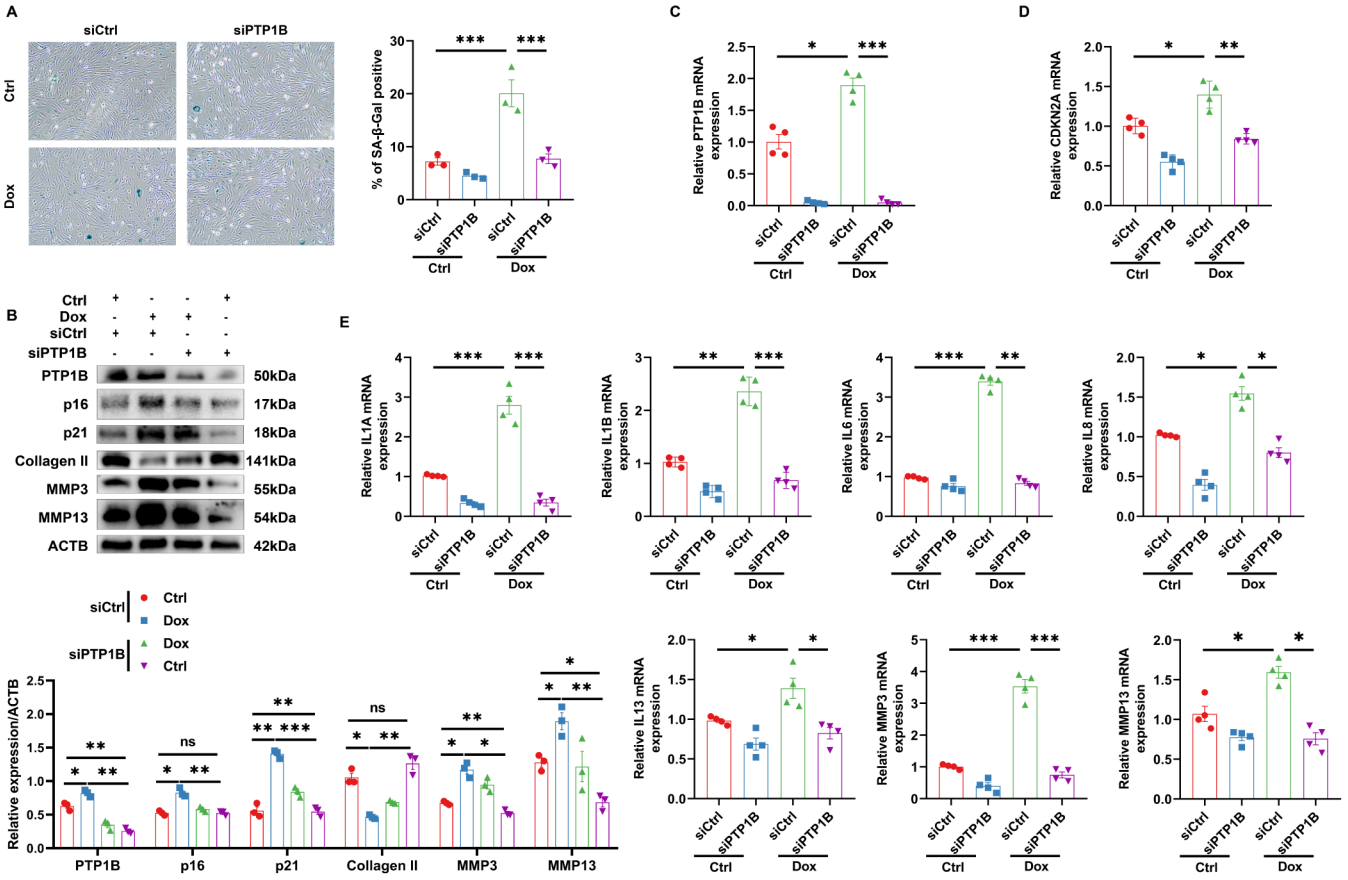

Figure 8. Knockdown of PTP1B inhibits chondrocyte senescence. (A) The typical images of the SA-β-Gal stained C28/I2 cells from the control and the dox group treated with or without siRNA targeting PTP1B (siPTP1B), as well as the subsequent quantification of the SA-β-Gal staining C28/I2 cells. $n = 3$, scale bar, 200 μm; (B) representative Western blot and quantification of PTP1B, p16, p21, Collagen II, MMP3, and MMP13 in C28/I2 cells derived from control and dox group treated with or without siPTP1B, $n = 3$; (C) qPCR analysis of mRNA levels of PTP1B in C28/I2 cells derived from control and dox group treated with or without si-PTP1B, $n = 4$, $^{*}p < 0.05$, $^{***}p < 0.001$; (D) qPCR analysis of mRNA levels of CDKN2A in C28/I2 cells derived from control and dox group treated with or without siPTP1B, $n = 4$; (E) qPCR analysis of mRNA levels of SASP-related inflammatory cytokines (IL-1α, IL-1β, IL-6, IL-8, and IL-13), MMP3 and MMP13 in C28/I2 cells derived from control and dox group treated with or without si-PTP1B, $n = 4$, $^{*}p < 0.05$, $^{**}p < 0.01$, $^{***}p < 0.001$; all data were presented as the means ± SEM. One-way analysis of variance with Dunnett's multiple comparisons was used for statistical analysis.

CONCLUSION

In conclusion, we showed that PTP1B knockdown prevented the senescence of chondrocytes and prevented cartilage degradation in OA. To the best of our knowledge, this study is the first to show a connection between PTP1B and chondrocyte senescence in OA chondrocytes. These findings offer a fresh perspective on the pathophysiology of OA, opening up new avenues for OA clinical diagnosis and targeted treatment.

ASSOCIATED CONTENT

Data Availability Statement

Original data are available from corresponding authors: zjewwei@zju.edu.cn and tengchong1984@zju.edu.cn. This paper does not report the original code. Any additional information required to reanalyze the data reported in this paper is available from the lead contact upon request. The links of the GEO data sets used in the present study were listed as follows: 1. GSE158875: https://www.ncbi.nlm.nih.gov/geo/query/acc.cgi?acc=GSE158875.

Supporting Information

The Supporting Information is available free of charge at https://pubs.acs.org/doi/10.1021/acsomega.3c10313.

1. DEGs were found in GSE158875 (PDF)

AUTHOR INFORMATION

Corresponding Authors

Wei Wei − *Department of Orthopedics, the Fourth Affiliated Hospital of School of Medicine, and International School of Medicine, International Institutes of Medicine, Zhejiang University, Yiwu, Zhejiang 322000, PR China; Key Laboratory of Tissue Engineering and Regenerative Medicine of Zhejiang Province, Zhejiang University School of Medicine, Hangzhou, Zhejiang 310000, PR China;* orcid.org/0000-0002-2234-4459; Email: zjewwei@zju.edu.cn

Chong Teng − *Department of Orthopedics, the Fourth Affiliated Hospital of School of Medicine, and International School of Medicine, International Institutes of Medicine, Zhejiang University, Yiwu, Zhejiang 322000, PR China;* orcid.org/0009-0008-7850-669X; Email: tengchong1984@zju.edu.cn

https://doi.org/10.1021/acsomega.3c10313
ACS Omega 2024, 9, 27017−27029

Authors

Hui-Min Li − *Department of Orthopedics, the Fourth Affiliated Hospital of School of Medicine, and International School of Medicine, International Institutes of Medicine, Zhejiang University, Yiwu, Zhejiang 322000, PR China;* orcid.org/0000-0002-6846-2610

Xianda Che − *Department of Orthopedics, The Second Hospital of Shanxi Medical University, Taiyuan, Shanxi 030001, PR China*

Zhicheng Tong − *Department of Orthopedics, the Fourth Affiliated Hospital of School of Medicine, and International School of Medicine, International Institutes of Medicine, Zhejiang University, Yiwu, Zhejiang 322000, PR China*

Complete contact information is available at: https://pubs.acs.org/10.1021/acsomega.3c10313

Author Contributions

#H.-M.L. and X.C. are contributed equally to the work and should be regarded as cofirst authors; H.-M.L., W.W., and C.T. designed the study. H.-M.L. and Z.T. performed the experiments. H.-M.L. and Z.T. performed the statistical analysis. H.-M.L., W.W., and C.T. drafted the article. H.-M.L., W.W., and C.T. supervised the experimental work. All authors contributed to the article and approved the submitted version.

Notes

The authors declare no competing financial interest.

■ ABBREVIATIONS

OA	osteoarthritis
PTP1B	protein tyrosine phosphatase 1B
GEO	gene expression omnibus
GO	gene ontology
IGF1	insulin-like growth factor 1
DEGs	differential expressed genes
SA-β-Gal	senescence-associated β-galactosidase

■ REFERENCES

(1) Loeser, R. F.; Goldring, S. R.; Scanzello, C. R.; Goldring, M. B. Osteoarthritis: a disease of the joint as an organ. *Arthritis Rheumatol.* **2012**, *64* (6), 1697−1707.

(2) Hootman, J. M.; Helmick, C. G. Projections of US prevalence of arthritis and associated activity limitations. *Arthritis Rheumatol.* **2006**, *54* (1), 226−229.

(3) Hunter, D. J.; Bierma-Zeinstra, S. Osteoarthritis. *Lancet* **2019**, *393* (10182), 1745−1759.

(4) Huang, C.; Zou, K.; Wang, Y.; Tang, K.; Wu, Y. Esculetin Alleviates IL-1β-Evoked Nucleus Pulposus Cell Death, Extracellular Matrix Remodeling, and Inflammation by Activating Nrf2/HO-1/NF-kb. *ACS Omega* **2024**, *9* (1), 817−827.

(5) Sun, S.; Wang, Y.; Li, J.; Wu, A.; Xie, Y.; Wang, Z.; Zhao, X.; Wang, D.; Wu, X.; Liu, X. Network Pharmacology-Based Approach to Investigate the Active Ingredients and Therapeutic Mechanisms of Jingu Tongxiao Pill against Osteoarthritis. *ACS Omega* **2023**, *8* (34), 31529−31540.

(6) Pitou, M.; Papi, R. M.; Tzavellas, A.-N.; Choli-Papadopoulou, T. ssDNA-Modified Gold Nanoparticles as a Tool to Detect miRNA Biomarkers in Osteoarthritis. *ACS Omega* **2023**, *8* (8), 7529−7535.

(7) Xiong, W.; Zhao, J.; Ma, X.; Feng, Z. Mechanisms and Molecular Targets of BuShenHuoXue Formula for Osteoarthritis. *ACS Omega* **2022**, *7* (5), 4703−4713.

(8) Li, H. M.; Liu, Y.; Zhang, R. J.; Ding, J. Y.; Shen, C. L. Vitamin D receptor gene polymorphisms and osteoarthritis: a meta-analysis. *Rheumatology* **2021**, *60* (2), 538−548.

(9) Martel-Pelletier, J.; Barr, A. J.; Cicuttini, F. M.; Conaghan, P. G.; Cooper, C.; Goldring, M. B.; Goldring, S. R.; Jones, G.; Teichtahl, A. J.; Pelletier, J. -P. Osteoarthritis. *Nat. Rev. Dis. Primers* **2016**, *2*, 16072.

(10) Prieto-Alhambra, D.; Judge, A.; Javaid, M. K.; Cooper, C.; Diez-Perez, A.; Arden, N. K. Incidence and risk factors for clinically diagnosed knee, hip and hand osteoarthritis: influences of age, gender and osteoarthritis affecting other joints. *Ann. Rheum. Dis.* **2014**, *73* (9), 1659−1664.

(11) Lotz, M.; Loeser, R. F. Effects of aging on articular cartilage homeostasis. *Bone* **2012**, *51* (2), 241−248.

(12) Mobasheri, A.; Matta, C.; Zákány, R.; Musumeci, G. Chondrosenescence: definition, hallmarks and potential role in the pathogenesis of osteoarthritis. *Maturitas* **2015**, *80* (3), 237−244.

(13) Chen, X.; Gong, W.; Shao, X.; Shi, T.; Zhang, L.; Dong, J.; Shi, Y.; Shen, S.; Qin, J.; Jiang, Q.; et al. METTL3-mediated m 6 A modification of ATG7 regulates autophagy-GATA4 axis to promote cellular senescence and osteoarthritis progression. *Ann. Rheum. Dis.* **2022**, *81* (1), 87−99.

(14) Wolfenson, H.; Yang, B.; Sheetz, M. P. Steps in Mechanotransduction Pathways that Control Cell Morphology. *Annu. Rev. Physiol.* **2019**, *81*, 585−605.

(15) Yin, W.; Park, J. I.; Loeser, R. F. Oxidative stress inhibits insulin-like growth factor-I induction of chondrocyte proteoglycan synthesis through differential regulation of phosphatidylinositol 3-Kinase-Akt and MEK-ERK MAPK signaling pathways. *J. Biol. Chem.* **2009**, *284* (46), 31972−31981.

(16) Loeser, R. F.; Gandhi, U.; Long, D. L.; Yin, W.; Chubinskaya, S. Aging and oxidative stress reduce the response of human articular chondrocytes to insulin-like growth factor 1 and osteogenic protein 1. *Arthritis Rheumatol.* **2014**, *66* (8), 2201−2209.

(17) Loeser, R. F.; Collins, J. A.; Diekman, B. O. Ageing and the pathogenesis of osteoarthritis. *Nat. Rev. Rheumatol.* **2016**, *12* (7), 412−420.

(18) Buckley, D. A.; Cheng, A.; Kiely, P. A.; Tremblay, M. L.; O'Connor, R. Regulation of insulin-like growth factor type I (IGF-I) receptor kinase activity by protein tyrosine phosphatase 1B (PTP-1B) and enhanced IGF-I-mediated suppression of apoptosis and motility in PTP-1B-deficient fibroblasts. *Mol. Cell. Biol.* **2002**, *22* (7), 1998−2010.

(19) Kenner, K. A.; Anyanwu, E.; Olefsky, J. M.; Kusari, J. Protein-tyrosine phosphatase 1B is a negative regulator of insulin- and insulin-like growth factor-I-stimulated signaling. *J. Biol. Chem.* **1996**, *271* (33), 19810−19816.

(20) Lopez-Otin, C.; Blasco, M. A.; Partridge, L.; Serrano, M.; Kroemer, G. The hallmarks of aging. *Cell* **2013**, *153* (6), 1194−1217.

(21) Sun, C.; Zhang, F.; Ge, X.; Yan, T.; Chen, X.; Shi, X.; Zhai, Q. SIRT1 improves insulin sensitivity under insulin-resistant conditions by repressing PTP1B. *Cell Metab.* **2007**, *6* (4), 307−319.

(22) Gagarina, V.; Gabay, O.; Dvir-Ginzberg, M.; Lee, E. J.; Brady, J. K.; Quon, M. J.; Hall, D. J. SirT1 enhances survival of human osteoarthritic chondrocytes by repressing protein tyrosine phosphatase 1B and activating the insulin-like growth factor receptor pathway. *Arthritis Rheumatol.* **2010**, *62* (5), 1383−1392.

(23) Lagouge, M.; Argmann, C.; Gerhart-Hines, Z.; Meziane, H.; Lerin, C.; Daussin, F.; Messadeq, N.; Milne, J.; Lambert, P.; Elliott, P.; et al. Resveratrol improves mitochondrial function and protects against metabolic disease by activating SIRT1 and PGC-1alpha. *Cell* **2006**, *127* (6), 1109−1122.

(24) Li, H. M.; Liu, Y.; Ding, J. Y.; Zhang, R.; Liu, X. Y.; Shen, C. L. In silico Analysis Excavates A Novel Competing Endogenous RNA Subnetwork in Adolescent Idiopathic Scoliosis. *Front. Med.* **2020**, *7*, 583243.

(25) Tong, Z.; Li, H.; Jin, Y.; Sheng, L.; Ying, M.; Liu, Q.; Wang, C.; Teng, C. Mechanisms of ferroptosis with immune infiltration and inflammatory response in rotator cuff injury. *Genomics* **2023**, *115*, 110645.

(26) Ding, Z.; Liu, Y.; Huang, Q.; Cheng, C.; Song, L.; Zhang, C.; Cui, X.; Wang, Y.; Han, Y.; Zhang, H. m6A- and immune-related

lncRNA signature confers robust predictive power for immune efficacy in lung squamous cell carcinoma. *View* **2023**, *4*, 20220083.
(27) Han, X.; Cai, L.; Lu, Y.; Li, D.; Yang, J. Identification of tRNA-derived fragments and their potential roles in diabetic cataract rats. *Epigenomics* **2020**, *12* (16), 1405−1418.
(28) Villanueva, R. A. M.; Chen, Z. J. *ggplot2: elegant graphics for data analysis*, Taylor & Francis, 2019.
(29) Subramanian, A.; Tamayo, P.; Mootha, V. K.; Mukherjee, S.; Ebert, B. L.; Gillette, M. A.; Paulovich, A.; Pomeroy, S. L.; Golub, T. R.; Lander, E. S.; et al. Gene set enrichment analysis: a knowledge-based approach for interpreting genome-wide expression profiles. *Proc. Natl. Acad. Sci. U. S. A.* **2005**, *102* (43), 15545−15550.
(30) Liberzon, A.; Subramanian, A.; Pinchback, R.; Thorvaldsdóttir, H.; Tamayo, P.; Mesirov, J. P. Molecular signatures database (MSigDB) 3.0. *Bioinformatics* **2011**, *27* (12), 1739−1740.
(31) Castanza, A. S.; Recla, J. M.; Eby, D.; Thorvaldsdóttir, H.; Bult, C. J.; Mesirov, J. P. Extending support for mouse data in the Molecular Signatures Database (MSigDB). *Nat. Methods* **2023**, *20* (11), 1619−1620.
(32) Kuleshov, M. V.; Jones, M. R.; Rouillard, A. D.; Fernandez, N. F.; Duan, Q.; Wang, Z.; Koplev, S.; Jenkins, S. L.; Jagodnik, K. M.; Lachmann, A.; et al. Enrichr: a comprehensive gene set enrichment analysis web server 2016 update. *Nucleic Acids Res.* **2016**, *44*, W90−W97.
(33) Xu, X.; Zhang, Q.; Li, M.; Lin, S.; Liang, S.; Cai, L.; Zhu, H.; Su, R.; Yang, C. Microfluidic single-cell multiomics analysis. *VIEW* **2023**, *4* (1), 20220034.
(34) Szklarczyk, D.; Morris, J. H.; Cook, H.; Kuhn, M.; Wyder, S.; Simonovic, M.; Santos, A.; Doncheva, N. T.; Roth, A.; Bork, P.; et al. The STRING database in 2017: quality-controlled protein-protein association networks, made broadly accessible. *Nucleic Acids Res.* **2017**, *45* (D1), D362−D368.
(35) Song, H.; Wang, H.; Zhu, J. VIEW the future of biodiagnostics. *VIEW* **2020**, *1* (1), No. e2.
(36) Goldring, M. B.; Birkhead, J. R.; Suen, L. F.; Yamin, R.; Mizuno, S.; Glowacki, J.; Arbiser, J. L.; Apperley, J. F. Interleukin-1 beta-modulated gene expression in immortalized human chondrocytes. *J. Clin. Invest.* **1994**, *94* (6), 2307−2316.
(37) Zhu, J.; Yang, S.; Qi, Y.; Gong, Z.; Zhang, H.; Liang, K.; Shen, P.; Huang, Y. Y.; Zhang, Z.; Ye, W.; et al. Stem cell−homing hydrogel-based miR-29b-5p delivery promotes cartilage regeneration by suppressing senescence in an osteoarthritis rat model. *Sci. Adv.* **2022**, *8* (13), No. eabk0011.
(38) Yue, L.; Berman, J. What Is Osteoarthritis? *Jama* **2022**, *327* (13), 1300.
(39) Zhang, C.; Cheng, Z.; Zhou, Y.; Yu, Z.; Mai, H.; Xu, C.; Zhang, J.; Wang, J. The novel hyaluronic acid granular hydrogel attenuates osteoarthritis progression by inhibiting the TLR-2/NF-κB signaling pathway through suppressing cellular senescence. *Bioeng. Transl. Med.* **2023**, *8* (3), No. e10475.
(40) Zhang, H.; Shao, Y.; Yao, Z.; Liu, L.; Zhang, H.; Yin, J.; Xie, H.; Li, K.; Lai, P.; Zeng, H.; et al. Mechanical overloading promotes chondrocyte senescence and osteoarthritis development through downregulating FBXW7. *Ann. Rheum. Dis.* **2022**, *81* (5), 676−686.
(41) Zhang, J.; Zhu, J.; Zhao, B.; Nie, D.; Wang, W.; Qi, Y.; Chen, L.; Li, B.; Chen, B. LTF induces senescence and degeneration in the meniscus via the NF-κB signaling pathway: A study based on integrated bioinformatics analysis and experimental validation. *Front. Mol. Biosci.* **2023**, *10*, 1134253.
(42) Chen, Y. -H.; Zhang, X.; Chou, C. -H.; Hsueh, M. -F.; Attarian, D.; Li, Y. -J.; Kraus, V. B. Association of Dipeptidylpeptidase 4 (CD26) With Chondrocyte Senescence and Radiographic Progression in Knee Osteoarthritis. *Arthritis Rheumatol.* **2023**, *75*, 1120−1131.
(43) Alonso, A.; Sasin, J.; Bottini, N.; Friedberg, I.; Friedberg, I.; Osterman, A.; Godzik, A.; Hunter, T.; Dixon, J.; Mustelin, T. Protein tyrosine phosphatases in the human genome. *Cell* **2004**, *117* (6), 699−711.
(44) Tonks, N. K. Protein tyrosine phosphatases: from genes, to function, to disease. *Nat. Rev. Mol. Cell Biol.* **2006**, *7* (11), 833−846.
(45) Moller, D. E. New drug targets for type 2 diabetes and the metabolic syndrome. *Nature* **2001**, *414* (6865), 821−827.
(46) Bakhtiyari, S.; Meshkani, R.; Taghikhani, M.; Larijani, B.; Adeli, K. Protein tyrosine phosphatase-1B (PTP-1B) knockdown improves palmitate-induced insulin resistance in C2C12 skeletal muscle cells. *Lipids* **2010**, *45* (3), 237−244.
(47) Elchebly, M.; Payette, P.; Michaliszyn, E.; Cromlish, W.; Collins, S.; Loy, A. L.; Normandin, D.; Cheng, A.; Himms-Hagen, J.; Chan, C. C.; et al. Increased insulin sensitivity and obesity resistance in mice lacking the protein tyrosine phosphatase-1B gene. *Science* **1999**, *283* (5407), 1544−1548.
(48) Loeser, R. F. Aging and osteoarthritis: the role of chondrocyte senescence and aging changes in the cartilage matrix. *Osteoarthritis Cartilage* **2009**, *17* (8), 971−979.
(49) Gabay, O.; Zaal, K. J.; Sanchez, C.; Dvir-Ginzberg, M.; Gagarina, V.; Song, Y.; He, X. H.; McBurney, M. W. Sirt1-deficient mice exhibit an altered cartilage phenotype. *Joint Bone Spin* **2013**, *80* (6), 613−620.
(50) Zhu, J.; An, Y.; Wang, X.; Huang, L.; Kong, W.; Gao, M.; Wang, J.; Sun, X.; Zhu, S.; Xie, Z. The natural product rotundic acid treats both aging and obesity by inhibiting PTP1B. *Life Med.* **2022**, *1* (3), 372−386.
(51) Ibrayeva, A.; Bay, M.; Pu, E.; Jörg, D. J.; Peng, L.; Jun, H.; Zhang, N.; Aaron, D.; Lin, C.; Resler, G.; et al. Early stem cell aging in the mature brain. *Cell Stem Cell* **2021**, *28* (5), 955−966.e7.
(52) Lin, A. W.; Barradas, M.; Stone, J. C.; van Aelst, L.; Serrano, M.; Lowe, S. W. Premature senescence involving p53 and p16 is activated in response to constitutive MEK/MAPK mitogenic signaling. *Genes Dev.* **1998**, *12* (19), 3008−3019.

https://doi.org/10.1021/acsomega.3c10313
ACS Omega 2024, 9, 27017−27029